Quantized Control Under Round-Robin Communication Protocol

Kun Liu, *Member, IEEE*, Emilia Fridman, *Senior Member, IEEE*, Karl Henrik Johansson, *Fellow, IEEE*, and Yuanqing Xia, *Senior Member, IEEE*

***Abstract*—This paper analyzes the exponential stability of a discrete-time linear plant in feedback control over a communication network with N sensor nodes, dynamic quantization, large communication delays, variable sampling intervals, and round-robin scheduling. The closed-loop system is modeled as a switched system with multiple-ordered time-varying delays and bounded disturbances. We propose a time-triggered zooming algorithm implemented at the sensors that preserves exponential stability of the closed-loop system. A direct Lyapunov approach is presented for initialization of the zoom variable. The proposed framework can be applied to the plants with polytopic type uncertainties. The effectiveness of the method is illustrated on cart-pendulum and quadruple-tank processes.**

***Index Terms*—Dynamic quantization, Lyapunov method, networked control systems (NCSs), round-robin protocol, switched time-delay systems.**

I. Introduction

THE rapidly developing wireless communication technology enables networked control systems (NCSs) with increased flexibility, ease of installation, and reduced costs [9], [26]. In many such systems, the transmissions are constrained by bandwidth limitations and interference [3], [7], [33].

In such systems, one of the constraints associated with control over communication networks is that only a subset of sensors and actuators can transmit their data over the channel at each transmission instant. Therefore, protocols are needed to schedule which node is given access to the network at each time instant. There are three main classes of scheduling protocols: 1) periodic protocols, of which round-robin is a special case [7], [20], [21]; 2) quadratic protocols, which include try-once-discard protocol [7], [20], [21], [30]; and 3) stochastic protocols [2], [3], [18], [28].

Manuscript received March 1, 2015; revised September 23, 2015, November 30, 2015, December 26, 2015, and January 9, 2016; accepted February 10, 2016. Date of publication March 8, 2016; date of current version June 9, 2016. This work was supported in part by the National Natural Science Foundation of China under Grant 61503026 and Grant 61440058, in part by the Israel Science Foundation under Grant 1128/14, in part by the Knut and Alice Wallenberg Foundation, and in part by the Swedish Research Council.

K. Liu and Y. Xia are with the School of Automation, Beijing Institute of Technology, Beijing 100081, China (e-mail: kunliubit@bit.edu.cn; xia_yuanqing@bit.edu.cn).

E. Fridman is with the School of Electrical Engineering, Tel-Aviv University, Tel-Aviv 69978, Israel (e-mail: emilia@eng.tau.ac.il).

K. H. Johansson is with the ACCESS Linnaeus Centre and School of Electrical Engineering, KTH Royal Institute of Technology, SE-100 44 Stockholm, Sweden (e-mail: kallej@kth.se).

Color versions of one or more of the figures in this paper are available online at http://ieeexplore.ieee.org.

Digital Object Identifier 10.1109/TIE.2016.2539259

Another communication constraint is that transmitted data should be quantized before they are sent from the sensor to the controller/actuator [11], [32], [34]. Quantization is implemented by a device that converts a real-valued signal into a piecewise constant one with a finite set of values. Quantized control has been paid considerable attention in recent years. When the system is affected by a static quantizer, a simple approach is to treat the quantization interval as uncertainty [6], [25], and to bound the uncertainty by using the sector bound approach [5]. Dynamic quantization was proposed in [1], where the quantizer incorporated an adjustable "zoom" variable. General types of dynamic quantizers were studied in [11]–[13].

By simultaneously considering dynamic quantization and scheduling protocols, a unified framework was provided in [20] for the analysis of NCSs via a hybrid system approach. However, delays were not included in the analysis. A linear matrix inequality (LMI)-based time-triggered zooming algorithm was presented in [17] via a time-delay system approach for NCSs with dynamic quantization and variable communication delays. As pointed out in [17], taking communication delays into consideration leads to additional challenges: 1) the closed-loop system and the resulting solution bounds should be formulated in terms of updating time instants at the actuators, while the zooming algorithm should be given in terms of sampling instants at the sensors; and 2) the solution bounds should include additional bounds on the first time interval of the delay length [15]. In [17], the zooming algorithm was proposed in terms of sampling instants at the sensors and a direct Lyapunov approach was presented for initialization of the zoom variable. However, scheduling protocols were not taken into account. This observation and the need for scheduling in wireless NCSs motivate us to develop a time-delay system approach for linear NCSs under scheduling and dynamic quantization.

In this paper, we consider the stability analysis of discrete-time NCSs with N sensor nodes. The system involves dynamic quantization, large communication delays, variable sampling intervals, and round-robin scheduling protocol. The closed-loop quantized system is modeled as a switched system with multiple and ordered time-varying delays and bounded disturbances. In the presence of the round-robin protocol, a time-triggered zooming algorithm, which is implemented at the sensors, is proposed and it is shown to lead to an exponentially stable closed-loop system. After each zooming-in instant, we suggest waiting for all the N latest transmitted measurements to arrive at the controller side and then sending them together to the actuator side. Following [15], we present a direct Lyapunov

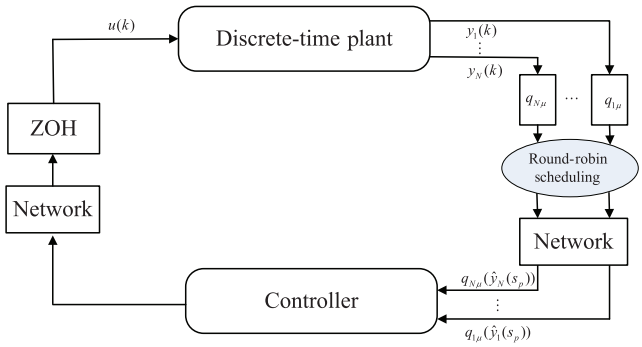

Fig. 1. NCSs with quantizers and round-robin scheduling.

approach for initialization of the zoom variable. Polytopic type uncertainties in the plant model can be easily incorporated in the framework.

This paper is organized as follows. Section II defines the model of the considered quantized discrete-time NCSs under round-robin scheduling. An input-to-state stability (ISS) condition is derived by a Lyapunov method for the switched closed-loop system model. Based on this ISS condition, Section III proposes an LMI-based zooming algorithm for the dynamic quantization. It is shown that it leads to exponential stability of the closed-loop system. Two illustrative examples are discussed in Section IV. The conclusion and future work are finally stated in Section V.

Notations: The superscript "T" stands for matrix transposition, $\mathbb{R}^n$ denotes the n-dimensional Euclidean space with vector norm $|\cdot|$, $\mathbb{R}^{n\times m}$ is the set of all $n\times m$ real matrices, and the notation $P>0$, for $P\in\mathbb{R}^{n\times n}$ means that P is symmetric and positive definite. The symbol $*$ represents the symmetric term of a symmetric matrix. $\mathbb{Z}^+$ and $\mathbb{N}$ denote the set of nonnegative and positive integers, respectively. $\lfloor x\rfloor$ denotes the largest integer k such that $k\le x$, i.e., $\lfloor x\rfloor=\max\{k\in\mathbb{Z}:k\le x\}$. $\lceil x\rceil$ denotes the smallest integer k such that $k\ge x$, i.e., $\lceil x\rceil=\min\{k\in\mathbb{Z}:k\ge x\}$.

II. NCS Model and Problem Formulation

In this section, we present the considered discrete-time NCS model and some preliminary results on the problem to be solved in this paper.

A. Quantized NCS Under Round-Robin Scheduling

The quantized NCS is depicted schematically in Fig. 1. It consists of a linear discrete-time plant, N distributed sensors and quantizers, a controller node and an actuator node, which are all connected via communication networks. The discrete-time plant is given by

$$x(k+1)=Ax(k)+Bu(k),\quad k\in\mathbb{Z}^+ \tag{1}$$

where $x(k)\in\mathbb{R}^n$ denotes the state of the plant, and $u(k)\in\mathbb{R}^{n_u}$ the control input. The matrices A and B may be certain or uncertain. The initial condition is given by $x(0)=x_0$. It is assumed that x_0 may be unknown, but satisfies the bound $|x_0|<X_0$, where $X_0>0$ is known. The assumption on boundedness of the initial state is common, e.g., for interval observer design [23].

The measurement outputs of the plant are described by $y_i(k)=C_ix(k)\in\mathbb{R}^{n_i}$, $i=1,\dots,N$, $\sum_{i=1}^N n_i=n_y$. We denote $C=\left[\begin{array}{ccc}C_1^T&\cdots&C_N^T\end{array}\right]^T$, $y(k)=\left[\begin{array}{ccc}y_1^T(k)&\cdots&y_N^T(k)\end{array}\right]^T\in\mathbb{R}^{n_y}$. Following [6], we consider the quantization effect from the sensors to the controller.

Let $z_i(k)\in\mathbb{R}^{n_i}$, $i=1,\dots,N$, be the vectors to be quantized. The quantizers are piecewise constant functions $q_i(z_i(k))$: $\mathbb{R}^{n_i}\to\mathbb{D}_i$, where $\mathbb{D}_i$ is a finite subset of $\mathbb{R}^{n_i}$, $i=1,\dots,N$. It is assumed that there exist real numbers $M_i>\Delta_i>0$, $i=1,\dots,N$, such that the following two conditions hold:

1) if $|z_i(k)|\le M_i$, then $|q_i(z_i(k))-z_i(k)|\le\Delta_i$;
2) if $|z_i(k)|>M_i$, then $|q_i(z_i(k))|>M_i-\Delta_i$

where Δ_i and M_i are the quantization interval bounds and ranges, respectively. Condition 1) gives a bound on the quantization interval when the quantizer does not saturate, and condition 2) provides a way to detect saturation.

We consider quantized measurements as in [11]

$$q_{i\mu}(z_i(k)):=\mu(k)q_i\left(\frac{z_i(k)}{\mu(k)}\right),\ i=1,\dots,N \tag{2}$$

where $\mu(k)>0$ is the zoom variable. The range of the quantizer $q_{i\mu}$ is $\mu(k)M_i$ and the quantization interval is $\mu(k)\Delta_i$, $i=1,\dots,N$. The zoom variable $\mu(k)$ changes dynamically to achieve exponential stability.

Let s_p represent the unbounded and monotonously increasing sequence of sampling instants, i.e.,

$$\begin{array}{l}0=s_0<s_1<\cdots<s_p<\cdots,\ p\in\mathbb{Z}^+\\ \lim\limits_{p\to\infty}s_p=\infty,\ s_{p+1}-s_p\le\text{MATI}\end{array} \tag{3}$$

where $\{s_p\}$ is a subsequence of $\mathbb{Z}^+$ and MATI denotes the maximum allowable transmission interval. Denote by $q_\mu(\hat y(s_p))=[q_{1\mu}^T(\hat y_1(s_p))\ \cdots\ q_{N\mu}^T(\hat y_N(s_p))]^T\in\mathbb{R}^{n_y}$ the output information submitted to the scheduling protocol. At each sampling instant s_p, one of the outputs $y_i(s_p)\in\mathbb{R}^{n_i}$ is quantized and transmitted over the network, i.e., one of the $q_{i\mu}(\hat y_i(s_p))$ values is updated with the recent quantized output $q_{i\mu}(y_i(s_p))$. Let $i_p^*\in\mathcal{I}=\{1,\dots,N\}$ denote the active output node at the sampling instant s_p, which will be chosen according to the scheduling protocol below.

Consider round-robin scheduling for the choice of the active quantized output node: $q_{i\mu}(y_i(k))=q_{i\mu}(C_ix(k))$, $k\in\mathbb{Z}^+$, is transmitted only at the sampling instant $k=s_{N\ell+i-1}$, $\ell\in\mathbb{Z}^+$, $i=1,\dots,N$. After each transmission and reception, the values in $q_{i\mu}(y_i(k))$ are updated with the newly received values, while the values of $q_{j\mu}(y_j(k))$ for $j\ne i$ remain the same, as no additional information is received. This leads to the constrained data exchange expressed as

$$q_{i\mu}(\hat y_i(s_p))=\left\{\begin{array}{ll}q_{i\mu}(y_i(s_p))=q_{i\mu}(C_ix(s_p)), & p=N\ell+i-1,\\ q_{i\mu}(\hat y_i(s_{p-1})), & p\ne N\ell+i-1,\end{array}\right.\ \ell\in\mathbb{Z}^+. \tag{4}$$

It is assumed that data packet loss does not occur. Denote by t_p the updating time instant of the zero-order holder (ZOH). Suppose that the updating data at the instant t_p on the actuator side has experienced a variable transmission delay $\eta_p = t_p - s_p$. As in [19], the delays may be either smaller or larger than the sampling interval provided that the transmission order of data packets is maintained. Assume that the network-induced delay η_p and the time span between the updating and the current sampling instants are bounded

$$t_{p+1} - 1 - t_p + \eta_p \le \tau_M^N, \quad 0 \le \eta_m \le \eta_p \le \eta_M,\ p \in \mathbb{Z}^+ \tag{5}$$

where τ_M^N, η_m, and η_M are known nonnegative integers. Then, we have

$$\begin{aligned}(t_{p+1}-1) - s_p &= s_{p+1} - s_p + \eta_{p+1} - 1\\ &\le \text{MATI} + \eta_M - 1 = \tau_M^N\\ (t_{p+1}-1) - s_{p-N+j} &= s_{p+1} - s_{p-N+j} + \eta_{p+1} - 1\\ &\le (N-j+1)\text{MATI} + \eta_M - 1\\ &= (N-j+1)\tau_M^N - (N-j)\eta_M\\ &\quad + N - j \triangleq \tau_M^j,\ j = 1,\dots,N-1\\ t_{p+1} - t_p &\le \tau_M^N - \eta_m + 1.\end{aligned} \tag{6}$$

B. Switched System Model

Next, we introduce a switched system model as the closed-loop system of NCS provided above. Suppose that the controller and the actuator are event-driven. The most recent output information on the controller side is denoted by $q_\mu(\hat{y}(s_p))$. Assume that there exists a matrix $K = [K_1 \ \dots \ K_N]$, $K_i \in \mathbb{R}^{m\times n_i}$ such that $A + BKC$ is Schur stable. Consider the static output feedback controller

$$u(k) = Kq_\mu(\hat{y}(s_p)), \quad k \in [t_p, t_{p+1} - 1],\ k \in \mathbb{Z}^+. \tag{7}$$

Due to (4), the controller (7) can be represented as

$$\begin{aligned}u(k) &= K_{i_p^*} q_{i_p^*\mu}(y_{i_p^*}(t_p - \eta_p))\\ &\quad + \sum_{i=1, i\neq i_p^*}^{N} K_i q_{i\mu}(\hat{y}_i(t_{p-1} - \eta_{p-1})), \quad k \in [t_p, t_{p+1}-1]\end{aligned} \tag{8}$$

where i_p^* is the index of the active node at s_p and η_p is the communication delay. The closed-loop system with round-robin scheduling is modeled as a switched system

$$\begin{aligned}x(k+1) &= Ax(k) + \sum_{j=1}^{N} A_{\theta(i,j)} x(t_{p-N+j} - \eta_{p-N+j})\\ &\quad + \sum_{j=1}^{N} B_{\theta(i,j)} \omega_{\theta(i,j)}(k), \quad k \in [t_p, t_{p+1}-1],\ i = 1,\dots,N\end{aligned} \tag{9}$$

where $A_{\theta(i,j)} = BK_{\theta(i,j)}C_{\theta(i,j)}$, $B_{\theta(i,j)} = BK_{\theta(i,j)}$

$$p = \begin{cases} N\ell + i - 1, & \text{for } i \in \mathcal{I}\backslash\{N\},\ \ell \in \mathbb{N}\\ N\ell - 1, & \text{for } i = N,\ \ell \in \mathbb{N}\end{cases}$$

$$\theta(i,j) = \begin{cases} i + j, & \text{if } i + j \le N,\\ i + j - N, & \text{if } i + j > N,\ j = 1,\dots,N\end{cases}$$

and

$$\begin{aligned}\omega_{\theta(i,j)}(k) &= q_{\theta(i,j)\mu}(y_{\theta(i,j)}(s_{p-N+j})) - y_{\theta(i,j)}(s_{p-N+j})\\ &\quad i \in \mathcal{I},\ j = 1,\dots,N\end{aligned}$$

denote the quantization intervals. If $|y_{\theta(i,j)}(s_{p-N+j})| \le \mu(k)M_{\theta(i,j)}$, then $|\omega_{\theta(i,j)}(k)| \le \mu(k)\Delta_{\theta(i,j)}$, $i \in \mathcal{I}$, $j = 1,\dots,N$, for $k \in [t_p, t_{p+1} - 1]$.

We represent $t_{p-N+j} - \eta_{p-N+j} = k - \tau_j(k)$, $j = 1,\dots,N$, where

$$\begin{aligned}&\tau_\vartheta(k) < \tau_{\vartheta-1}(k), \quad \vartheta = 2,\dots,N\\ &\tau_\vartheta(k) = k - t_{p-N+\vartheta} + \eta_{p-N+\vartheta}\\ &\tau_{\vartheta-1}(k) = k - t_{p-N+\vartheta-1} + \eta_{p-N+\vartheta-1}\\ &\tau_j(k) \in [\eta_m, \tau_M^j], \quad k \in [t_p, t_{p+1} - 1],\ j = 1,\dots,N.\end{aligned} \tag{10}$$

Therefore, (9) can be considered as a system with N time-varying interval delays, where $\tau_\vartheta(k) < \tau_{\vartheta-1}(k)$, $\vartheta = 2,\dots,N$.

The objective of this paper is to find an LMI-based time-triggered zooming algorithm [i.e., to choose a suitable time-varying parameter $\mu(k)$] for exponential stability of the switched system (9). To do so, we first present a lemma for ISS of system (9) with static quantization [i.e., $\mu(k) \equiv \mu$]. This lemma plays a key role in achieving the main results.

C. ISS Under Round-Robin Scheduling and Static Quantization

Definition 1: The switched system (9) is said to be ISS if there exist constants $b > 0$, $0 < \kappa < 1$ and $b' > 0$ such that, for initial condition $x_{t_{N-1}} \in \underbrace{\mathbb{R}^n \times \cdots \times \mathbb{R}^n}_{\tau_M^1 + 1 \text{ times}}$ and for disturbances ω_i, $i = 1,\dots,N$, the solutions of the switched system (9) satisfy

$$\begin{aligned}|x(k)|^2 &\le b\kappa^{2(k-t_{N-1})}\|x_{t_{N-1}}\|_c^2\\ &\quad + b' \max\{|\omega(t_{N-1})|^2, \dots, |\omega(k)|^2\},\ k \ge t_{t_{N-1}}\end{aligned}$$

where $\|x_{t_{N-1}}\|_c = \sup_{t_{N-1} - \tau_M^1 \le s \le t_{N-1}} |x(s)|$ and $\omega = col\{\omega_1, \dots, \omega_N\}$.

Consider first static quantizers with a constant zoom variable $\mu(k) \equiv \mu$. We apply the following discrete-time Lyapunov functional to (9) with time-varying delay from the maximum delay interval $[\eta_m, \tau_M^1]$ [4]

$$\begin{aligned}V(x_k) &= x^T(k)Px(k) + \sum_{s=k-\eta_m}^{k-1} \lambda^{k-s-1} x^T(s) S_0 x(s)\\ &\quad + \eta_m \sum_{j=-\eta_m}^{-1} \sum_{s=k+j}^{k-1} \lambda^{k-s-1} \eta^T(s) R_0 \eta(s)\\ &\quad + \sum_{s=k-\tau_M^1}^{k-\eta_m-1} \lambda^{k-s-1} x^T(s) S_1 x(s)\\ &\quad + (\tau_M^1 - \eta_m) \sum_{j=-\tau_M^1}^{-\eta_m-1} \sum_{s=k+j}^{k-1} \lambda^{k-s-1} \eta^T(s) R_1 \eta(s)\\ &\eta(k) = x(k+1) - x(k),\\ &P > 0,\ S_i > 0,\ R_i > 0,\ i = 0, 1,\ 0 < \lambda < 1\end{aligned} \tag{11}$$

where $x_k(j) \triangleq x(k+j),\ j=-\tau_M^1,\dots,-1,0$, and $x(k)=x_0,\ k=-\tau_M^1,\dots,-1,0$. Following [4], we find conditions such that

$$V(x_{k+1})-\lambda V(x_k)-\sum_{i=1}^{N} b_i|\omega_i(k)|^2\le 0,\quad k\ge t_{N-1} \tag{12}$$

holds, where $0<\lambda<1$, $b_i>0$, $i=1,\dots,N$. Then, we arrive at the following conditions to guarantee (12) and thus, for ISS of the switched system (9).

Lemma 1: Given scalar $0<\lambda<1$, positive integers $0\le \eta_m<\tau_M^N$, and K_i, $i=1,\dots,N$, assume that there exist scalars $b_i>0,\ i=1,\dots,N$, $n\times n$ matrices $P>0,\ S_i>0,\ R_i>0,\ i=0,1,\ G_{\ell,\vartheta}^i\ i=1,\dots,N,\ \ell=1,\dots,N,\ \vartheta=2,\dots,N+1,\ \ell<\vartheta$, such that the following LMIs are feasible:

$$\Omega_i=\begin{bmatrix} R_1 & * \\ (G_{\ell,\vartheta}^i)^T & R_1\end{bmatrix}\ge 0 \tag{13}$$

$$\begin{bmatrix} \Psi & * & * \\ PF_0^i & -P & * \\ H(F_0^i-F_1) & 0 & -H\end{bmatrix}<0 \tag{14}$$

where

$$\begin{aligned}
&F_0^i=[A\ 0_{n\times n}\ A_{\theta(i,N)}\dots A_{\theta(i,1)}\ 0_{n\times n}\ B_{\theta(i,N)}\dots B_{\theta(i,1)}]\\
&F_1=[I_n\ 0_{n\times((N+2)n+n_y)}],\ F_2=[0_{n\times n}\ I_n\ 0_{n\times((N+1)n+n_y)}],\\
&\quad\dots,\ F_{N+3}=[0_{n\times((N+2)n)}\ I_n\ \ 0_{n\times n_y}]\\
&\Sigma=\mathrm{diag}\{S_0-\lambda P,-\lambda^{\eta_m}(S_0-S_1),0_{(Nn)\times(Nn)},-\lambda^{\tau_M^1}S_1,\\
&\quad -b_{\theta(i,N)}I_{\theta(i,N)},\dots,-b_{\theta(i,1)}I_{\theta(i,1)}\}\\
&\Psi=\Sigma-\lambda^{\eta_m}(F_1-F_2)^TR_0(F_1-F_2)\\
&\quad -\lambda^{\tau_M^1}\sum_{i=2}^{N+2}(F_i-F_{i+1})^TR_1(F_i-F_{i+1})\\
&\quad -2\lambda^{\tau_M^1}\sum_{j=2}^{N+1}(F_j-F_{j+1})^T\sum_{s=j+1}^{N+2}G_{j-1,s-1}^i(F_s-F_{s+1})\\
&H=\eta_m^2R_0+(\tau_M^1-\eta_m)^2R_1,\quad i=1,\dots,N.
\end{aligned} \tag{15}$$

Let $\mu>0$ be a constant and $|\omega_i(k)|\le\mu\Delta_i,\ i=1,\dots,N$. Then, the solutions of the switched system (9) with the initial conditions $x_{t_{N-1}}\in\underbrace{\mathbb{R}^n\times\cdots\times\mathbb{R}^n}_{\tau_M^1+1\text{ times}}$ satisfy the following inequalities:

$$V(x_k)\le\lambda^{k-t_{N-1}}V(x_{t_{N-1}})+\frac{\mu^2}{1-\lambda}\sum_{i=1}^{N}b_i\Delta_i^2,\ k\ge t_{N-1}. \tag{16}$$

Proof: See the Appendix. ∎

In order to derive a bound on $V(t_{N-1})$ in terms of x_0 in a simple way, we suggest waiting for all the N latest transmitted measurements $q_{1\mu}(y_1(s_0))$, $q_{2\mu}(y_2(s_1)),\dots,q_{N\mu}(y_N(s_{N-1}))$ on the controller side and then sending them together to the actuator side. This is a reasonable approach which can be easily implemented. Then for $k=0,1,\dots,t_{N-1}-1$, (1) is given by

$$x(k+1)=Ax(k),\quad k=0,1,\dots,t_{N-1}-1. \tag{17}$$

Remark 1: A common Lyapunov functional (11) has been applied to the switched system (9) to derive sufficient conditions for ISS. It should be pointed out that the multiple Lyapunov functional method and dwell time approach can be utilized to find a suitable switching signal to improve performance [8], [27].

III. Main Results: Dynamic Quantization of NCSs Under Round-Robin Scheduling

In the following, based on ISS of system (9), we present the main results on dynamic quantization of NCSs in the presence of round-robin scheduling. By defining the initial and level sets in Section III-A, in Section III-B, we propose an LMI-based time-triggered zooming algorithm for exponential stability of the switched system (9). In Section III-C, we develop a novel Lyapunov-based method to initialize the zoom parameter. Under the round-robin protocol scheduling, digit "1" is transmitted in the protocol along with the measurements at the zooming-in sampling instants (otherwise, digit "0" is transmitted). Thus, on the controller side, it is known whether the zoom variable μ of the received measurement is updated or not. Once the value of μ is updated, all N latest transmitted measurements are waited on the controller side and then sent together to the actuator side.

A. Initial and Level Sets

Given positive numbers σ and ρ, the initial and level sets are defined as

$$\begin{aligned}
\mathcal{S}_\sigma=\{x_{t_{N-1}}\in\underbrace{\mathbb{R}^n\times\cdots\times\mathbb{R}^n}_{\tau_M^1+1\text{ times}}:\ &V(x_{t_{N-1}})<\sigma,\\
&x^T(k)Px(k)<\sigma,\ k\in[t_{N-1}-\eta_M,t_{N-1}]\}
\end{aligned} \tag{18}$$

and

$$\mathcal{X}_{k^*,\rho}=\{x_k\in\underbrace{\mathbb{R}^n\times\ldots\times\mathbb{R}^n}_{\tau_M^1+1\text{ times}}:V(x_k)<\rho,k=k^*,k^*+1,\dots\}$$

respectively. Given positive numbers μ, M_0, $\beta<1$ and $\nu<1$, the following lemma ensures that all solutions of (9) with $x_{t_{N-1}}\in\mathcal{S}_{\mu^2M_0^2}$ stay inside the region $\mathcal{X}_{t_{N-1},(1+\beta\nu^2)\mu^2M_0^2}$ for all $k\ge t_{N-1}$, and enter a smaller region $\mathcal{X}_{t_{N-1}+T,\nu^2\mu^2M_0^2}$ in a finite time T.

Lemma 2: Given $M_j>0,\ j=0,1,\dots,N,\ \Delta_i>0,\ i=1,\dots,N$, positive integers $0\le\eta_m<\tau_M^N$ and tuning parameters $0<\lambda<1$, $0<\nu<1$, assume that there exist scalars $0<\beta<1$, $b_i,\ i=1,\dots,N$, $n\times n$ matrices $P>0,\ S_i>0,\ R_i>0,\ i=0,1,\ G_{\ell,j}^i\ i=1,\dots,N,\ \ell=1,\dots,N,\ j=2,\dots,N+1,\ \ell<j$, such that LMIs (13) and (14) and

$$(1+\beta\nu^2)M_0^2C_i^TC_i<PM_i^2,\ i=1,\dots,N \tag{19}$$

$$\frac{1}{1-\lambda}\sum_{i=1}^{N}b_i\Delta_i^2<\beta\nu^2M_0^2 \tag{20}$$

hold. Let $\mu>0$ be a constant. Then, the solutions of (9) that start in the region $\mathcal{S}_{\mu^2M_0^2}$

1) satisfy $|C_ix(t_p-\eta_p)|=|y_i(t_p-\eta_p)|<\mu M_i$, $p\in\mathbb{Z}^+$, (implying $|\omega_i(k)|\le\mu\Delta_i$ for all $i\in\mathcal{I}$ and $k=t_{N-1},t_{N-1}+1,\dots$);

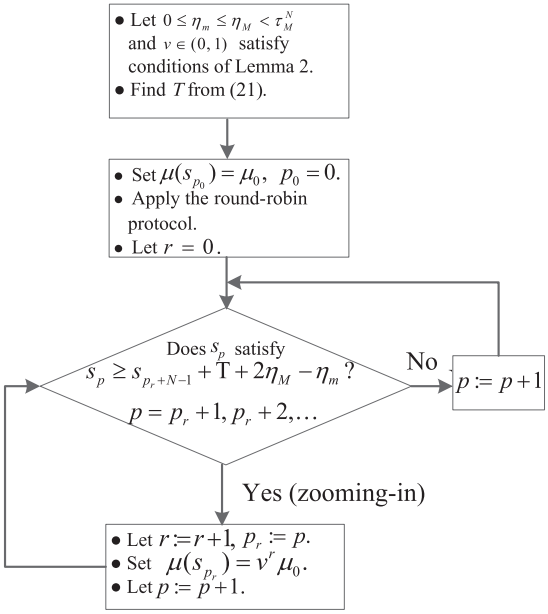

Fig. 2. Algorithm for dynamic quantization and round-robin scheduling.

2) remain in the set $\mathcal{X}_{t_{N-1},(1+\beta\nu^2)\mu^2 M_0^2}$;
3) enter a smaller set $\mathcal{X}_{t_{N-1}+T,\nu^2\mu^2 M_0^2}$ in a finite time $T = \lceil \tilde{T} \rceil$, where $\tilde{T}$ is the solution of

$$\lambda^{\tilde{T}} = (1-\beta)\nu^2. \tag{21}$$

The proof of Lemma 2 follows from [17]. The second inequality in (18) allows us to guarantee the bounds on $y(s_p)$, $s_p < t_{N-1}$ by verifying (19).

Remark 2: The functional $V(x_k)$ is a standard Lyapunov functional for delay-dependent analysis. The LMIs of Lemma 2 are feasible for small enough delay bound τ_M^N, large enough quantization ranges $M_1, \ldots, M_N$, and small enough quantization intervals $\Delta_1, \ldots, \Delta_N$. Indeed, the LMIs (13) and (14) are feasible for $\tau_M^N = 0$ (i.e., in the absence of delay) since $A + BKC$ is Schur stable. Hence, (13) and (14) are feasible for small enough τ_M^N. The LMIs (19) and (20) are feasible for large enough quantization ranges and small enough quantization intervals. Moreover, the initial values of λ and ν can be set to be 1. It is noted that the conditions are sufficient only and always may be improved.

B. Dynamic Quantization and Zooming Algorithm

In this section, we consider dynamic quantizers with the zoom variable μ. Zooming is performed on the sensor level. Therefore, in the closed-loop system, $\mu = \mu(s_p)$ is constant on $[t_p, t_{p+1} - 1]$.

Given $\mu_0 > 0$, let $\mu = \mu_0$, $x_{t_{N-1}} \in \mathcal{S}_{\mu^2 M_0^2} = \mathcal{S}_{\mu_0^2 M_0^2}$. We will show how to choose μ_0 in Theorem 1 below. Assume that LMIs of Lemma 2 are feasible. In the sequel, we propose a zooming-in algorithm in Fig. 2, where μ is decreased and thus, the resulting quantization interval is reduced to drive the state of (9) to the origin exponentially.

Definition 2: If there exist constants $b > 0$ and $0 < \kappa < 1$ such that

$$|x(k)|^2 \le b\kappa^{2(k-t_{N-1})}\mu_0^2 M_0^2 \quad \forall k \ge t_{N-1},\ k \in \mathbb{N}$$

for the solutions of the system (9) initialized with $x_{t_{N-1}} \in \mathcal{S}_{\mu_0^2 M_0^2}$, then the system (9) with $|\omega_i(k)| \le \mu\Delta_i$, $i = 1, \ldots, N$, is said to be exponentially stable with decay rate κ for some choice of the zoom variable $\mu > 0$.

Proposition 1: Assume that the LMIs of Lemma 2 are feasible. Given $\mu_0 > 0$, let $\mu = \mu_0$, $x_{t_{N-1}} \in \mathcal{S}_{\mu_0^2 M_0^2}$. Then under the algorithm in Fig. 2, the system (9) is exponentially stable with a decay rate $\kappa = \nu^{\frac{1}{\bar{\tau}_M}}$, where

$$\bar{\tau}_M = T + N\tau_M^N + 2\eta_M - N\eta_m - \eta_m + N. \tag{22}$$

Proof: Set $r = 0$. Since

$$t_{p_1} - \eta_M = s_{p_1} + \eta_{p_1} - \eta_M \ge t_{N-1} + T + \eta_{p_1} - \eta_m \ge t_{N-1} + T$$

application of Lemma 2 with $\mu = \mu_0$ leads to

$$x^T(k)Px(k) \le V(x_k) < \nu^2\mu_0^2 M_0^2 \quad \forall k \ge t_{p_1} - \eta_M,\ k \in \mathbb{N}.$$

Set $r = 1$. We wait for all N latest transmitted measurements to arrive into the reduced domain with $x^T(s_p)C_i^T C_i x(s_p) < \mu_0^2\nu^2 M_i^2$, $i = 1, \ldots, N$ for $p \ge p_1$, where $|\omega_i(k)| \le \mu_0\nu\Delta_i$, $k \ge t_{p_1}$, $k \in \mathbb{N}$. After sampling instant s_{p_1+N-1}, the resulting closed-loop system has initial condition

$$x_{t_{p_1+N-1}} \in \underbrace{\mathbb{R}^n \times \cdots \times \mathbb{R}^n}_{\tau_M^1+1 \text{ times}} : V(x_{t_{p_1+N-1}}) < \nu^2\mu_0^2 M_0^2. \tag{23}$$

Then, Lemma 2 is applied with $\mu = \mu_0\nu$, where t_{N-1} and η_{N-1} are changed by t_{p_1+N-1} and η_{p_1+N-1}, respectively. Thus, the solutions of (9) initiated by (23) remain in a region $\mathcal{X}_{t_{p_1+N-1},(1+\beta\nu^2)\nu^2\mu_0^2 M_0^2}$ for all $k \ge t_{p_1+N-1}$, $k \in \mathbb{N}$. Since $s_{p_1+N-1} = t_{p_1+N-1} - \eta_{p_1+N-1} \ge t_{p_1+N-1} - \eta_M$, from (19) it follows that:

$$x^T(s_p)C_i^T C_i x(s_p) < \frac{x^T(s_p)Px(s_p)\cdot\nu^2\mu_0^2 M_i^2}{(1+\beta\nu^2)\nu^2\mu_0^2 M_0^2} < \nu^2\mu_0^2 M_i^2,$$
$$i = 1, \ldots, N \quad \forall p \ge p_1 + N - 1$$

and thus, $|\omega_i(k)| \le \nu\mu_0\Delta_i, i = 1, \ldots, N$, $k \ge t_{p_1+N-1} = s_{p_1+N-1} + \eta_{p_1+N-1}$. Therefore, for $k \ge t_{p_2} - \eta_M \ge t_{p_1+N-1} + T$

$$\begin{aligned} V(x_k) &\le \lambda^{k-t_{p_1+N-1}} V(x_{t_{p_1+N-1}}) + \frac{\nu^2\mu_0^2}{1-\lambda}\sum_{i=1}^N b_i\Delta_i^2 \\ &\le \lambda^T V(x_{t_{p_1+N-1}}) + \frac{\nu^2\mu_0^2}{1-\lambda}\sum_{i=1}^N b_i\Delta_i^2 \\ &< (1-\beta)\nu^2\cdot\nu^2\mu_0^2 M_0^2 + \beta\nu^2\mu_0^2 M_0^2\cdot\nu^2 \\ &= \nu^4\mu_0^2 M_0^2. \end{aligned}$$

Similarly, for $r = 2, 3, \ldots$ we have $V(x_k) < \nu^{2r}\mu_0^2 M_0^2$ for all $k \in [t_{p_r} - \eta_M, t_{p_{r+1}} - \eta_M - 1]$. Noting that

$$rT + (r-1)(2\eta_M - \eta_m + N - 1) + t_{N-1} \le t_{p_r} - \eta_M$$
$$\le k \le t_{p_{r+1}} - \eta_M - 1 < (r+1)\bar{\tau}_M - 1 + t_{N-1}$$

we obtain

$$\begin{aligned} V(x_k) &< \nu^{2r}\mu_0^2M_0^2 < \nu^{2\left(\frac{k-t_{N-1}}{\bar\tau_M}-\frac{\bar\tau_M-1}{\bar\tau_M}\right)}\mu_0^2M_0^2 \\ &= \nu^{-\frac{2(\bar\tau_M-1)}{\bar\tau_M}}\left(\nu^{\frac{1}{\bar\tau_M}}\right)^{2(k-t_{N-1})}\mu_0^2M_0^2, \\ & k\in[t_{p_r}-\eta_M, t_{p_{r+1}}-\eta_M-1],\ r\in\mathbb{N}. \end{aligned}$$

Then, the following holds for $k \geq t_{N-1}$:

$$\begin{aligned} |x(k)|^2 \leq\ & \nu^{-\frac{2(\bar\tau_M-1)}{\bar\tau_M}}[\lambda_{\min}(P)]^{-1} \\ & \times\left(\nu^{\frac{1}{\bar\tau_M}}\right)^{2(k-t_{N-1})}\mu_0^2M_0^2. \end{aligned}$$

■

Remark 3: In the above analysis, it is assumed that data packet dropout does not occur. However, for small delays $\eta_p < s_{p+1}-s_p$, if the number of successive packet dropouts is upper bounded by $\bar d$, in the presence of round-robin scheduling we could accommodate for packet dropouts by modeling them as prolongations of the transmission interval and replace T by $T+2\bar d\cdot$ MATI in the algorithm.

C. Initialization of the Zoom Variable

The algorithm of the previous section is given in terms of the initial set $\mathcal{S}_{\mu_0^2M_0^2}$ that involves the bound on $V(x_{t_{N-1}})$. In this section, we find the ball of initial conditions $x(0)=x_0$, starting from which the solutions of (9) and (17) remain in the initial set $\mathcal{S}_{\mu_0^2M_0^2}$. From (5) and the bound

$$\begin{aligned} s_{N-2} &= s_{N-2}-s_{N-3}+s_{N-3}-\cdots+s_1-s_0 \\ &\leq (N-2)(\tau_M^N-\eta_m+1) \end{aligned}$$

it holds that

$$\begin{aligned} t_{N-1} &\leq s_{N-2}+\tau_M^N+1 \\ &\leq (N-2)(\tau_M^N-\eta_m+1)+\tau_M^N+1 \triangleq \hat\tau_M. \end{aligned} \tag{24}$$

Then following [15], we derive a bound on $V(x_{t_{N-1}})$ in terms of x_0 in the next lemma:

Lemma 3: [15] Consider Lyapunov functional $V(x_k)$ given by (11) and denote $V_0(k)=x^T(k)Px(k)$. Under the constant initial condition $x(k)=x_0,\ k<0$, if there exist $0<\lambda<1$ and $c>1$ such that the following inequalities:

$$V_0(k+1)-cV_0(k)\leq 0 \tag{25a}$$

$$V(x_{k+1})-\lambda V(x_k)-(c-1)V_0(k)\leq 0 \tag{25b}$$

hold for $k=0,1,\ldots,t_{N-1}-1$ along (17), then we have

$$\begin{aligned} &V_0(k)\leq\lambda_{\max}(c^{\hat\tau_M}P)|x_0|^2,\quad k=0,1,\ldots,t_{N-1} \\ &V(x_{t_{N-1}})\leq\lambda_{\max}(c^{\hat\tau_M}P+\Omega)|x_0|^2 \end{aligned} \tag{26}$$

where $\hat\tau_M$ is given by (24) and

$$\Omega=\eta_mS_0+\lambda^{\eta_m}(\tau_M^1-\eta_m)S_1. \tag{27}$$

As a consequence, we achieve our main result:

Theorem 1: Given $M_j>0,\ j=0,1,\ldots,N,\ \Delta_i>0,\ i=1,\ldots,N$, positive integers $0\leq\eta_m\leq\eta_M<\tau_M^N$ and tuning parameters $0<\lambda<1,\ 0<\nu<1,\ c>1$, assume that there exist scalars $0<\beta<1, b_i,\ i=1,\ldots,N$, $n\times n$ matrices $P>0$, $S_i>0$, $R_i>0,\ i=0,1$, $G^i_{\ell,\vartheta}\ i=1,\ldots,N,\ \ell=1,\ldots,N$, $\vartheta=2,\ldots,N+1,\ \ell<\vartheta$, such that the LMIs (13) and (14), (19) and (20) and the following LMIs are feasible:

$$\begin{bmatrix} -cP & * \\ PA & -P \end{bmatrix}<0 \tag{28}$$

$$\begin{bmatrix} \tilde\Psi & * & * \\ P\tilde F_0 & -P & * \\ H(\tilde F_0-\tilde F_1) & 0 & -H \end{bmatrix}<0 \tag{29}$$

where

$$\begin{aligned} &\tilde F_0=[A\ 0_{n\times((N+2)n)}],\quad \tilde F_1=[I_n\ 0_{n\times((N+2)n)}] \\ &\tilde F_2=[0_{n\times n}\ I_n\ 0_{n\times((N+1)n)}],\ldots,\tilde F_{N+3}=[0_{n\times((N+2)n)}\ I_n] \\ &\tilde\Sigma=\mathrm{diag}\{S_0-\lambda P-(c-1)P, -\lambda^{\eta_m}(S_0-S_1), \\ &\qquad 0_{(Nn)\times(Nn)}, -\lambda^{\tau_M^1}S_1\} \\ &\tilde\Psi=\tilde\Sigma-\lambda^{\eta_m}(\tilde F_1-\tilde F_2)^TR_0(\tilde F_1-\tilde F_2) \\ &\quad -\lambda^{\tau_M^1}\sum_{i=2}^{N+2}(\tilde F_i-\tilde F_{i+1})^TR_1(\tilde F_i-\tilde F_{i+1}) \\ &\quad -2\lambda^{\tau_M^1}\sum_{j=2}^{N+1}(\tilde F_j-\tilde F_{j+1})^T\sum_{s=j+1}^{N+2}G^1_{j-1,s-1}(\tilde F_s-\tilde F_{s+1}) \end{aligned} \tag{30}$$

and the notation H is given by (15). If the initial condition satisfies the inequality $|x_0|<X_0$, where $X_0>0$ is known, then the zooming-in algorithm of Section III-B starting with $\mu(s_0)=\mu_0$ with μ_0 given by

$$\mu_0^2=\frac{\lambda_{\max}(c^{\hat\tau_M}P+\Omega)}{M_0^2}X_0^2 \tag{31}$$

exponentially stabilizes system (9) and (17), where $\hat\tau_M$ and Ω are given by (24) and (27), respectively.

Proof: From [15], it follows that the matrix inequalities (13), (28), and (29) guarantee (25) along (17) for $k=0,1,\ldots,t_{N-1}-1$. Therefore, if the initial condition satisfies the inequality $|x_0|<X_0$, then

$$\begin{aligned} \max\{V_0(k),V(x_{t_{N-1}})\} &\leq\lambda_{\max}(c^{\hat\tau_M}P+\Omega)X_0^2 \\ &=\mu_0^2M_0^2,\ k=0,1,\ldots,t_{N-1} \end{aligned}$$

meaning that $x_{t_{N-1}}\in\mathcal{S}_{\mu_0^2M_0^2}$. The result then follows from Proposition 1. ■

Remark 4: Note that given a bound $X_0>0$ on the state initial conditions and the values of the quantizer range $M_i>0$ and interval $\Delta_i>0,\ i=1,\ldots,N$, (31) defines the initial value of the zoom variable, starting from which the exponential stability is guaranteed by using zooming-in only. If the initial value of the zoom variable is given by μ_0, then the zooming-in algorithm of Section III-B starting with $\mu(s_0)=\mu_0$ exponentially stabilizes all the solutions of (9) and (17) starting from the initial ball

$$|x_0|<X_0,\quad X_0=\frac{\mu_0M_0}{\sqrt{\lambda_{max}(c^{\hat\tau_M}P+\Omega)}} \tag{32}$$

where $\hat\tau_M$ and Ω are given by (24) and (27), respectively. In order to maximize the initial ball (32), the condition $c^{\hat\tau_M}P+\Omega-\gamma I<0$ can be added to the conditions of Theorem 1, where $\gamma>0$ is to be minimized.

Remark 5: The conditions of Theorem 1 possess $(N+1)$ of $2n \times 2n$, one of $(N+5)n \times (N+5)n$, N of $((N+5)n+n_y) \times ((N+5)n+n_y)$ LMIs, and have the number $\frac{N^2(N+1)+5}{2}n^2+2.5n+N+1$ of decision variables. The huge numerical complexity is caused by the switched closed-loop system (9) composed of N subsystems.

Remark 6: The LMIs of Theorem 1 are affine in the system matrices. Therefore, in the case of system matrices from the uncertain time-varying polytope

$$\Theta = \sum_{j=1}^{M} g_j(k)\Theta_j, \quad 0 \le g_j(k) \le 1$$
$$\sum_{j=1}^{M} g_j(k) = 1, \quad \Theta_j = \left[\, A^{(j)} \;\; B^{(j)} \,\right]$$

where $g_j(k)$, $j = 1, \ldots, M$, are uncertain time-varying parameters and the system matrices $A^{(j)}$ and $B^{(j)}$, $j = 1, \ldots, M$, are known with appropriate dimensions, one has to solve these LMIs simultaneously for all the M vertices Θ_j, applying the same decision matrices.

Remark 7: The time-delay system approach has been developed in [16] and [18] for NCSs with nonquantized measurements under try-once-discard protocol and under stochastic protocol, respectively. The proposed zooming algorithm in the present paper for round-robin protocol could be extended to the case of try-once-discard and stochastic protocols. In addition, to facilitate the static output-feedback controller design, it will be useful to eliminate the coupling between the Lyapunov matrices and system matrices. To this end, one may resort to the methods proposed in, e.g., [24], and [35].

Remark 8: In a particular case of $N = 1$, the achieved conditions could be applied to the output tracking control that was studied in [14] and [31] for complex industrial processes. The discrete-time system theory for sampled-data control was applied in [14] and [31], whereas a time-delay approach is adopted in this paper.

IV. Illustrative Examples

A. Example 1: Inverted Pendulum

The inverted pendulum system is widely used as a benchmark for testing control algorithm. The dynamics of the inverted pendulum on a cart shown in Fig. 3 can be described in the following as in, e.g., [36]:

$$\begin{bmatrix} \dot{x} \\ \ddot{x} \\ \dot{\theta} \\ \ddot{\theta} \end{bmatrix} = \begin{bmatrix} 0 & 1 & 0 & 0 \\ 0 & -\frac{(a+ml^2)b}{a(M+m)+Mml^2} & -\frac{m^2gl^2}{a(M+m)+Mml^2} & 0 \\ 0 & 0 & 0 & 1 \\ 0 & -\frac{mlb}{a(M+m)+Mml^2} & -\frac{mgl(M+m)}{a(M+m)+Mml^2} & 0 \end{bmatrix} \begin{bmatrix} x \\ \dot{x} \\ \theta \\ \dot{\theta} \end{bmatrix} + \begin{bmatrix} 0 \\ \frac{a+ml^2}{a(M+m)+Mml^2} \\ 0 \\ \frac{ml}{a(M+m)+Mml^2} \end{bmatrix} u \tag{33}$$

with $M = 1.096$ kg, $m = 0.109$ kg, $l = 0.25$ m, $g = 9.8$ m/s^2, $a = 0.0034$ kg $\cdot$ m^2 and $b = 0.1$ N/m/s.

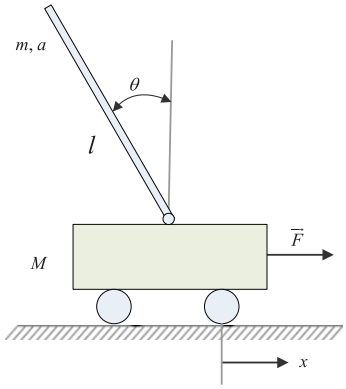

Fig. 3. Inverted pendulum system.

In the model, x, θ, a, and b represent cart position coordinate, pendulum angle from vertical, the friction of the cart, and inertia of the pendulum, respectively.

By choosing a sampling time $T_s = 0.01$ s, we obtain the following discrete-time system model:

$$x(k+1) = \begin{bmatrix} 1 & 0.01 & 0 & 0 \\ 0 & 0.9991 & 0.0063 & 0 \\ 0 & 0 & 1.0014 & 0.01 \\ 0 & -0.0024 & 0.2784 & 1.0014 \end{bmatrix} x(k) + \begin{bmatrix} 0 \\ 0.0088 \\ 0.0001 \\ 0.0236 \end{bmatrix} u(k), \; k \in \mathbb{Z}^+. \tag{34}$$

The pendulum can be stabilized by a state feedback $u(k) = Kx(k)$ with the gain $K = [K_1 \;\; K_2]$

$$K_1 = \left[\, 0.9163 \;\; 2.0169 \,\right], \quad K_2 = \left[\, -27.4850 \;\; -5.3437 \,\right]$$

which leads to the closed-loop system having eigenvalues $\{0.9419, 0.9865 + 0.0035i, 0.9865 - 0.0035i, 0.9813\}$. Suppose that the spatially distributed components of the state of the cart-pendulum system (34) are not accessible simultaneously.

Consider $N = 2$ and

$$C_1 = \begin{bmatrix} 1 & 0 & 0 & 0 \\ 0 & 1 & 0 & 0 \end{bmatrix}, \quad C_2 = \begin{bmatrix} 0 & 0 & 1 & 0 \\ 0 & 0 & 0 & 1 \end{bmatrix}. \tag{35}$$

The quantizer is chosen as

$$q_\mu(y^i) = \begin{cases} 100\mu \, \mathrm{sgn}(y^i), & \text{if } |y^i| > 100\mu \\ \mu \left\lfloor \frac{y^i}{\mu} + 0.01 \right\rfloor, & \text{if } |y^i| \le 100\mu \end{cases}$$

where y^i is the ith component of y, $i = 1, \ldots, 4$. Therefore, we can take $M_1 = M_2 = 100$, $\Delta_1 = \Delta_2 = 0.01$. Choose $\mu_0 = 1$, $M_0 = 100$, $\nu = 0.9$, $\lambda = 0.984$, $c = 1.37$, $\tau_M^N = 4$, $\eta_m = 0$, $\eta_M = 2$. Then from (5), it follows that the network-induced delays η_p and the sampling intervals are bounded by $0 \le \eta_p \le 2$ and $1 \le s_{p+1} - s_p \le 3$, $p \in \mathbb{Z}^+$, respectively. It is observed that we allow network-induced delays larger than the sampling intervals.

The initial state is assumed to be $x_0 = [0.5\, 0.3\, -0.2\, -0.9]^T$. In the simulation, the network-induced delays are

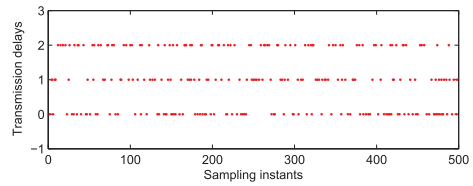

Fig. 4. Example 1: transmission delays.

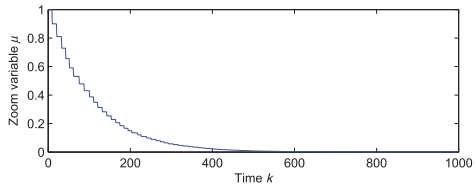

Fig. 5. Example 1: evolution of the zoom variable μ in the zooming-in algorithm.

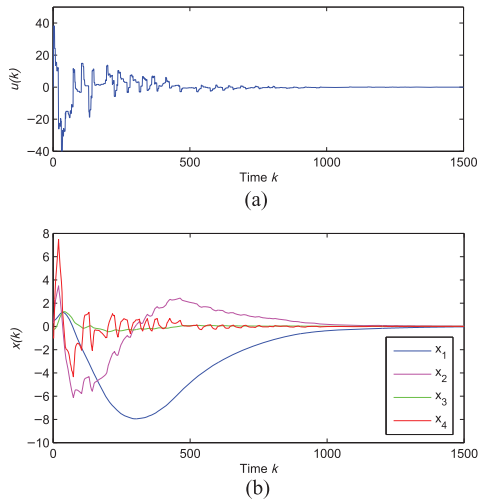

Fig. 6. Example 1: (a) evolution of the control input and (b) trajectory of the closed-loop system.

generated randomly according to the aforementioned assumption, and shown in Fig. 4. By Theorem 1, we find $T = \lceil -\frac{\ln(1-\beta)+2\ln\nu}{\ln\lambda} \rceil = 15$ from (21). Then, the zooming-in algorithm of Section III-B and round-robin protocol with $T = 15$ and $\nu = 0.9$ exponentially stabilizes all the solutions of (9) and (17) starting from the initial ball $|x_0| < 1.2376$. Fig. 5 shows the evolution of the zoom variable $\mu(k)$.

Moreover, it is found that the system is exponentially stable with a decay rate $\kappa = \nu^{\frac{1}{\bar{\tau}_M}} = 0.9964$, where [following (22)] $\bar{\tau}_M = T + 2\tau_M^N + 2\eta_M - 3\eta_m + 2 = 29$. The evolution of the control input and the state are depicted in Fig. 6.

For the case of $N = 1$, i.e., the scheduling is not taken into account and $y(k) = [C_1^T \;\; C_2^T]^T x(k)$, we achieve a slightly better $\kappa = 0.9950$ for essentially larger initial ball $|x_0| < 11.1951$.

B. Example 2: Quadruple-Tank Process

We also illustrate the efficiency of the given conditions on the example of the quadruple-tank process [10] described in Fig. 7. The linear discrete-time model obtained in [29] is

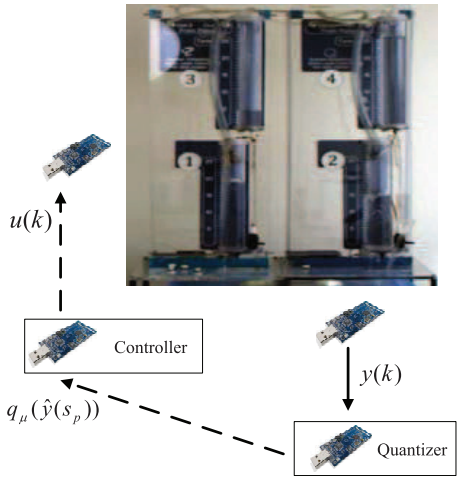

Fig. 7. Schematic diagram of the quadruple-tank process.

given by

$$x(k+1) = \begin{bmatrix} 0.975 & 0 & 0.042 & 0 \\ 0 & 0.977 & 0 & 0.044 \\ 0 & 0 & 0.958 & 0 \\ 0 & 0 & 0 & 0.956 \end{bmatrix} x(k) + \begin{bmatrix} 0.0515 & 0.0016 \\ 0.0019 & 0.0447 \\ 0 & 0.0737 \\ 0.0850 & 0 \end{bmatrix} u(k),\ k \in \mathbb{Z}^+. \quad (36)$$

Here, the open-loop system is exponentially stable with a decay rate $\kappa = 0.9770$.

Consider $N = 2$ and choose the controller gain $K = [K_1 \;\; K_2]$, where

$$K_1 = \begin{bmatrix} 0.0449 & -0.3007 \\ -0.3080 & 0.0469 \end{bmatrix}, \quad K_2 = \begin{bmatrix} 0.1651 & -0.5644 \\ -0.6275 & 0.1681 \end{bmatrix}.$$

The measurement outputs are $y_i(k) = C_i x(k)$ with C_i, $i = 1, 2$, given by (35). Suppose that the components of the state of system (36) are not accessible simultaneously. The quantizer is chosen as

$$q_\mu(y^i) = \begin{cases} 150\mu \operatorname{sgn}(y^i), & \text{if } |y^i| > 150\mu \\ \mu \left\lfloor \frac{y^i}{\mu} + 0.001 \right\rfloor, & \text{if } |y^i| \le 150\mu \end{cases}$$

where y^i is the ith component of y, $i = 1, \ldots, 4$. Therefore, we can take $M_1 = M_2 = 150$, $\Delta_1 = \Delta_2 = 0.001$.

Choose $\tau_M^N = 2$, $\eta_m = 0$, $\eta_M = 1$. From (5), it follows that the network-induced delays η_p and the sampling intervals are bounded by $0 \le \eta_p \le 1$ and $1 \le s_{p+1} - s_p \le 2$, $p \in \mathbb{Z}^+$, respectively. The network-induced delays are depicted in Fig. 8.

Then, we find that given $\mu_0 = 1$, $M_0 = 100$, $\nu = 0.1$, $\lambda = 0.926$, $c = 1.10$, the zooming-in algorithm of Section III-B and round-robin protocol with $T = 60$ exponentially stabilizes all the solutions of (9) and (17) starting from the initial ball $|x_0| < 23.7748$ with a decay rate $\kappa = 0.9667$. The decay rate for closed-loop system is improved compared to the one for the open-loop system. The evolution of the zoom variable $\mu(k)$ is presented in Fig. 9. The evolution of the control input and the

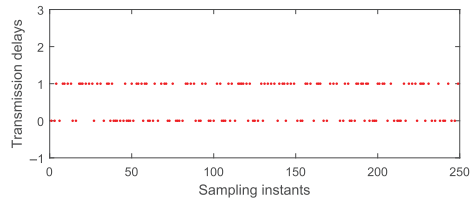

Fig. 8. Example 2: transmission delays.

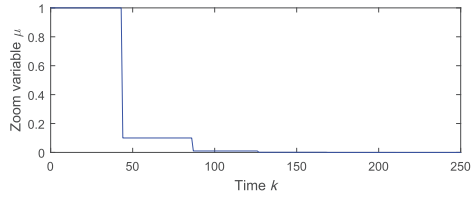

Fig. 9. Example 2: evolution of the zoom variable μ in the zooming-in algorithm.

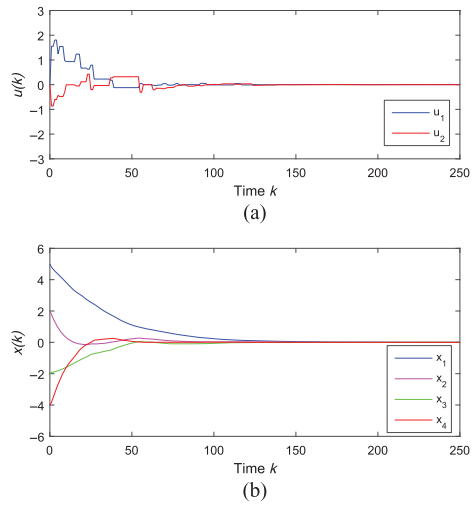

Fig. 10. Example 2: (a) evolution of the control input and (b) trajectory of the closed-loop system.

state with the initial state $x_0 = [5 \;\; 2 \;\; -2 \;\; -4]^T$ are given in Fig. 10.

Moreover, for the case of $N = 1$, it is shown that the zooming-in algorithm with $T = 60$ exponentially stabilizes all the solutions of the closed-loop system (9) and (17) ($N = 1$) starting from a larger initial ball $|x_0| < 91.4413$ with a slightly better decay rate $\kappa = 0.9647$.

V. Conclusion

This paper has investigated linear discrete-time NCSs that are subject to dynamic quantization, variable communication delays, variable sampling intervals, and round-robin scheduling. An LMI-based time-triggered zooming algorithm, which includes proper initialization of the zoom parameter, has been proposed for exponential stability of the switched closed-loop system. The interesting future research may include quantized input, stochastic communication delays, and dynamic scheduling protocols.

Appendix

Proof: Given $i \in \mathcal{I}$, consider $k \in [t_p, t_{p+1} - 1]$, $k \in \mathbb{Z}_+$ and define $\xi(k) = \text{col}\{x(k), x(k-\eta_m), x(k-\tau_N(k)), \ldots, x(k-\tau_1(k)), x(k-\tau_M^1), \omega_1(k), \ldots, \omega_N(k)\}$. Applying Cauchy–Schwarz inequality, taking advantage of the ordered delays and using convex analysis [22], we have

$$V(x_{k+1}) - \lambda V(x_k) - \sum_{i=1}^{N} b_i |\omega_i(k)|^2 \leq \xi^T(k)[\Psi + (F_0^i)^T P F_0^i + (F_0^i - F_1)^T H (F_0^i - F_1)]\xi(k) \leq 0 \tag{37}$$

if $\Psi + (F_0^i)^T P F_0^i + (F_0^i - F_1)^T H (F_0^i - F_1) < 0$, i.e., by Schur complement, if (14) is feasible.

Since $|\omega_i(k)| \leq \mu \Delta_i$, $i = 1, \ldots, N$, the inequality (37) implies for $k \in [t_p, t_{p+1} - 1]$

$$\begin{aligned} V(x_k) &\leq \lambda V(x_{k-1}) + \mu^2 \sum_{i=1}^{N} b_i \Delta_i^2 \\ &\vdots \\ &\leq \lambda^{k - t_{N-1}} V(x_{t_{N-1}}) + \frac{\mu^2}{1-\lambda} \sum_{i=1}^{N} b_i \Delta_i^2 \end{aligned}$$

that completes the proof. ■

References

[1] R. Brockett and D. Liberzon, "Quantized feedback stabilization of linear systems," *IEEE Trans. Automat. Control*, vol. 45, no. 7, pp. 1279–1289, Jul. 2000.

[2] M. Donkers, W. Heemels, D. Bernardini, A. Bemporad, and V. Shneer, "Stability analysis of stochastic networked control systems," *Automatica*, vol. 48, no. 5, pp. 917–925, May 2012.

[3] F. Farokhi and K. H. Johansson, "Stochastic sensor scheduling for networked control systems," *IEEE Trans. Automat. Control*, vol. 59, no. 5, pp. 1147–1162, May 2014.

[4] E. Fridman and M. Dambrine, "Control under quantization, saturation and delay: An LMI approach," *Automatica*, vol. 45, no. 10, pp. 2258–2264, Oct. 2009.

[5] M. Fu and L. Xie, "The sector bound approach to quantized feedback control," *IEEE Trans. Autoatm. Control*, vol. 50, no. 11, pp. 1698–1711, Nov. 2005.

[6] H. Gao, T. Chen, and J. Lam, "A new delay system approach to network-based control," *Automatica*, vol. 44, no. 1, pp. 39–52, Jan. 2008.

[7] W. Heemels, A. Teel, N. van de Wouw, and D. Nesic, "Networked control systems with communication constraints: Tradeoffs between transmission intervals, delays and performance," *IEEE Trans. Automat. Control*, vol. 55, no. 8, pp. 1781–1796, Aug. 2010.

[8] J. Hespanha and A. Morse, "Stability of switched systems with average dwell-time," in *Proc. 38th IEEE Conf. Decision Control*, Dec. 1999, pp. 2655–2660.

[9] J. Hespanha, P. Naghshtabrizi, and Y. Xu, "A survey of recent results in networked control systems," *Proc. IEEE*, vol. 95, no. 1, pp. 138–162, Jan. 2007.

[10] K. H. Johansson, "The quadruple-tank process: A multivariable laboratory process with an adjustable zero," *IEEE Trans. Control Syst. Technol.*, vol. 8, no. 3, pp. 456–465, Mar. 2000.

[11] D. Liberzon, "Hybrid feedback stabilization of systems with quantized signals," *Automatica*, vol. 39, no. 9, pp. 1543–1554, Sep. 2003.

[12] D. Liberzon, "Quantization, time delays, and nonlinear stabilization," *IEEE Trans. Automat. Control*, vol. 51, no. 7, pp. 1190–1195, Jul. 2006.

[13] D. Liberzon and D. Nesic, "Input-to-state stabilization of linear systems with quantized state measurements," *IEEE Trans. Automat. Control*, vol. 52, no. 5, pp. 767–781, May 2007.

[14] F. Liu, H. Gao, J. Qiu, S. Yin, J. Fan, and T. Chai, "Networked multirate output feedback control for setpoints compensation and its application to rougher flotation process," *IEEE Trans. Ind. Electron.*, vol. 61, no. 1, pp. 460–468, Jan. 2014.
[15] K. Liu and E. Fridman, "Delay-dependent methods and the first delay interval," *Syst. Control Lett.*, vol. 64, no. 1, pp. 57–63, Jan. 2014.
[16] K. Liu, E. Fridman, and L. Hetel, "Networked control systems in the presence of scheduling protocols and communication delays," *SIAM J. Control Optim.*, vol. 53, no. 4, pp. 1768–1788, Aug. 2015.
[17] K. Liu, E. Fridman, and K. H. Johansson, "Dynamic quantization of uncertain linear networked control systems," *Automatica*, vol. 59, pp. 248–255, Sep. 2015.
[18] K. Liu, E. Fridman, and K. H. Johansson, "Networked control with stochastic scheduling," *IEEE Trans. Automat. Control*, vol. 60, no. 11, pp. 3071–3076, Nov. 2015.
[19] P. Naghshtabrizi, J. Hespanha, and A. Teel, "Stability of delay impulsive systems with application to networked control systems," *Trans. Inst. Meas. Control*, vol. 32, no. 5, pp. 511–528, May 2010.
[20] D. Nesic and D. Liberzon, "A unified framework for design and analysis of networked and quantized control systems," *IEEE Trans. Automat. Control*, vol. 54, no. 4, pp. 732–747, Apr. 2009.
[21] D. Nesic and A. Teel, "Input–output stability properties of networked control systems," *IEEE Trans. Automat. Control*, vol. 49, no. 10, pp. 1650–1667, Oct. 2004.
[22] P. Park, J. Ko, and C. Jeong, "Reciprocally convex approach to stability of systems with time-varying delays," *Automatica*, vol. 47, no. 1, pp. 235–238, Jan. 2011.
[23] A. Polyakov, D. Efimov, W. Perruquetti, and J. P. Richard, "Output stabilization of time-varying input delay systems using interval observation technique," *Automatica*, vol. 49, no. 11, pp. 3402–3410, Nov. 2013.
[24] J. Qiu, G. Feng, and H. Gao, "Fuzzy-model-based piecewise static-output-feedback controller design for networked nonlinear systems," *IEEE Trans. Fuzzy Syst.*, vol. 18, no. 5, pp. 919–934, May 2010.
[25] J. Qiu, G. Feng, and H. Gao, "Observer-based piecewise affine output feedback controller synthesis of continuous-time T-S fuzzy affine dynamic systems using quantized measurements," *IEEE Trans. Fuzzy Syst.*, vol. 20, no. 6, pp. 1046–1062, Jun. 2012.
[26] Y. Shi, J. Huang, and B. Yu, "Robust tracking control of networked control systems: Application to a networked DC motor," *IEEE Trans. Ind. Electron.*, vol. 60, no. 12, pp. 5864–5874, Dec. 2013.
[27] X. Sun, J. Zhao, and D. Hill, "Stability and L_2-gain analysis for switched delay systems: A delay-dependent method," *Automatica*, vol. 42, no. 10, pp. 1769–1774, Oct. 2006.
[28] M. Tabbara and D. Nesic, "Input–output stability of networked control systems with stochastic protocols and channels," *IEEE Trans. Automat. Control*, vol. 53, no. 5, pp. 1160–1175, May 2008.
[29] A. Teixeira, "Toward cyber-secure and resilient networked control systems," Ph.D. dissertation, Automatic Control Lab., School Elect. Eng., KTH Royal Inst. Technol., Stockholm, Sweden, 2014.
[30] G. Walsh, H. Ye, and L. Bushnell, "Stability analysis of networked control systems," *IEEE Trans. Control Syst. Technol.*, vol. 10, no. 3, pp. 438–446, Mar. 2002.
[31] T. Wang, H. Gao, and J. Qiu, "A combined adaptive neural network and nonlinear model predictive control for multirate networked industrial process control," *IEEE Trans. Neural Netw. Learn. Syst.*, vol. 27, no. 2, pp. 416–425, Feb. 2016.
[32] Y. Xia, J. Yan, P. Shi, and M. Fu, "Stability analysis of discrete-time systems with quantized feedback and measurements," *IEEE Trans. Ind. Informat.*, vol. 9, no. 1, pp. 313–324, Jan. 2013.
[33] B. Xue, N. Li, S. Li, and Q. Zhu, "Moving horizon scheduling for networked control systems with communication constraints," *IEEE Trans. Ind. Electron.*, vol. 60, no. 8, pp. 3318–3327, Aug. 2013.
[34] C. Zhang, G. Feng, J. Qiu, and Y. Shen, "Control synthesis for a class of linear network-based systems with communication constraints," *IEEE Trans. Ind. Electron.*, vol. 60, no. 8, pp. 3339–3348, Aug. 2013.
[35] J. Zhang and Y. Xia, "Design of static output feedback sliding mode control for uncertain linear systems," *IEEE Trans. Ind. Electron.*, vol. 57, no. 6, pp. 2161–2170, Jun. 2010.
[36] J. Zhang, D. Zhao, and W. Zheng, "Output feedback control of discrete-time systems with self-triggered controllers," *Int. J. Robust Nonlinear Control*, vol. 25, no. 18, pp. 3698–3713, Dec. 2015.

Kun Liu (M'16) received the Ph.D. degree in electrical engineering and systems from Tel Aviv University, Tel Aviv, Israel, in 2012.

From February 2013 to February 2015, he was a Postdoctoral Researcher with the ACCESS Linnaeus Centre, KTH Royal Institute of Technology, Stockholm, Sweden. From March 2015 to August 2015, he held Researcher, Visiting, and Research Associate positions at, respectively, KTH Royal Institute of Technology, Stockholm, Sweden, CNRS, Laboratory for Analysis and Architecture of Systems, Toulouse, France, and The University of Hong Kong, Hong Kong. Since September 2015, he has been an Associate Professor with the School of Automation, Beijing Institute of Technology, Beijing, China. His research interests include time-delay systems, networked control, quantized systems, and robust control.

Emilia Fridman (M'12–SM'12) received the Ph.D. degree in mathematics from Voronezh State University, Voronezh, U.S.S.R., in 1986.

From 1986 to 1992, she was an Assistant and then an Associate Professor with the Department of Mathematics, Kuibyshev Institute of Railway Engineers, Kuibyshev, U.S.S.R. Since 1993, she has been with Tel Aviv University, Tel Aviv, Israel, where she is currently a Professor of Electrical Engineering Systems. She has held visiting positions at the Weierstrass Institute for Applied Analysis and Stochastics, Berlin, Germany, INRIA, Rocquencourt, France, Ecole Centrale de Lille, Lille, France, Valenciennes University, Valenciennes, France, University of Leicester, Leicester, U.K., University of Kent, Canterbury, U.K., CINVESTAV, Mexico City, Mexico, Zhejiang University, Hangzhou, China, St. Petersburg IPM, St. Petersburg, Russia, The University of Melbourne, Melbourne, Australia, Supelec, Paris, France, and KTH, Stockholm, Sweden. Her research interests include time-delay systems, networked control systems, distributed parameter systems, robust control, singular perturbations, and nonlinear control.

Prof. Fridman currently serves as an Associate Editor of *Automatica* and the *SIAM Journal on Control and Optimization*.

Karl Henrik Johansson (SM'08–F'12) received the M.Sc. and Ph.D. degrees in electrical engineering from Lund University, Lund, Sweden, in 1992 and 1997, respectively.

He is Director of the ACCESS Linnaeus Centre and a Professor with the School of Electrical Engineering, KTH Royal Institute of Technology, Stockholm, Sweden. He is a Wallenberg Scholar and has held a six-year Senior Researcher position with the Swedish Research Council. He is also heading the Stockholm Strategic Research Area ICT The Next Generation. He has held visiting positions at the University of California, Berkeley, CA, USA (1998–2000) and the California Institute of Technology, Pasadena, CA, USA (2006–2007). His research interests include networked control systems, cyber-physical systems, and applications in transportation, energy, and automation systems.

Dr. Johansson is currently on the Editorial Board of the IEEE TRANSACTIONS ON CONTROL OF NETWORK SYSTEMS and the *European Journal of Control*. He has been a Guest Editor for special issues, including one issue of the IEEE TRANSACTIONS ON AUTOMATIC CONTROL on cyber-physical systems and one of the *IEEE Control Systems Magazine* on cyber-physical security.

Yuanqing Xia (M'15–SM'16) received the Ph.D. degree in control theory and control engineering from Beijing University of Aeronautics and Astronautics, Beijing, China, in 2001.

From January 2002 to November 2003, he was a Postdoctoral Research Associate with the Institute of Systems Science, Academy of Mathematics and System Sciences, Chinese Academy of Sciences, Beijing, China. From November 2003 to February 2004, he was a Research Fellow with the National University of Singapore, Singapore, where he worked on variable structure control. From February 2004 to February 2006, he was a Research Fellow with the University of Glamorgan, Pontypridd, U.K. From February 2007 to June 2008, he was a Guest Professor with the Innsbruck Medical University, Innsbruck, Austria. Since 2004, he has been with the Department of Automatic Control, Beijing Institute of Technology, Beijing, China, first as an Associate Professor, then, since 2008, as a Professor. His research interests include networked control systems, robust control and signal processing, and active disturbance rejection control.